Development 125, 4821-4833 (1998)
Printed in Great Britain © The Company of Biologists Limited 1998
DEV4057

Math5 encodes a murine basic helix-loop-helix transcription factor expressed during early stages of retinal neurogenesis

Nadean L. Brown[1,2,*], Shami Kanekar[3], Monica L. Vetter[3], Priscilla K. Tucker[4], Debra L. Gemza[1,2] and Tom Glaser[1,2]

[1]Howard Hughes Medical Institute, [2]Departments of Human Genetics and Internal Medicine, and [4]Museum of Zoology and Department of Biology, University of Michigan, Ann Arbor, MI 48109-0650, USA
[3]Department of Neurobiology and Anatomy, University of Utah, Salt Lake City, UT 84132, USA
*Author for correspondence (e-mail: naybro@umich.edu)

Accepted 21 September; published on WWW 9 November 1998

SUMMARY

We have identified *Math5*, a mouse basic helix-loop-helix (bHLH) gene that is closely related to *Drosophila atonal* and *Xenopus Xath5* and is largely restricted to the developing eye. *Math5* retinal expression precedes differentiation of the first neurons and persists within progenitor cells until after birth. To position *Math5* in a hierarchy of retinal development, we compared *Math5* and *Hes1* expression in wild-type and *Pax6*-deficient (*Sey*) embryos. *Math5* expression is downregulated in *Sey/+* eyes and abolished in *Sey/Sey* eye rudiments, whereas the bHLH gene *Hes1* is upregulated in a similar dose-dependent manner. These results link *Pax6* to the process of retinal neurogenesis and provide the first molecular correlate for the dosage-sensitivity of the *Pax6* phenotype. During retinogenesis, *Math5* is expressed significantly before *NeuroD*, *Ngn2* or *Mash1*. To test whether these bHLH genes influence the fates of distinct classes of retinal neurons, we ectopically expressed *Math5* and *Mash1* in *Xenopus* retinal progenitors. Unexpectedly, lipofection of either mouse gene into the frog retina caused an increase in differentiated bipolar cells. Directed expression of *Math5*, but not *Xath5*, in *Xenopus* blastomeres produced an expanded retinal phenotype. We propose that *Math5* acts as a proneural gene, but has properties different from its most closely related vertebrate family member, *Xath5*.

Key words: Neuronal bHLH, Retina, Transcription, Proneural genes, Pax6, Mouse, Eye development

INTRODUCTION

Within the developing vertebrate central nervous system (CNS), cells undergo alterations in both morphology and gene expression as they differentiate. The retina is a good model for studying cell fate determination and differentiation in the CNS because it evaginates directly from the neural tube yet forms a relatively simple, laminated tissue. The retina is composed of a seven distinct cell types: retinal ganglion cells (RGCs), amacrine cells, bipolar cells, horizontal cells, rod and cone photoreceptor cells, and Müller glial cells, which originate from a uniform neuroepithelial sheet of cells. Mature retinal neurons and glia are stereotypically arranged in layers, which form as progenitor cells exit the cell cycle, migrate to the correct location and differentiate (Robinson, 1991). In vivo and in vitro studies suggest that retinal progenitor cell fate is influenced by both internal and external factors (Cepko et al., 1996). Each cell type emerges from the precursor population in an invariant temporal sequence. The differentiation status and birthdate of mature retinal cells are tightly correlated, implying that progenitors respond differently over time (Alexiades and Cepko, 1997; Wantanabe and Raff, 1990; Williams and Goldowitz, 1992). Environmental signals also affect the type of cell that a progenitor may become (Holt et al., 1988; Turner et al., 1987; Wetts and Fraser, 1988). While several intrinsic and extrinsic factors have been identified as possible differentiation cues (Furukawa et al., 1997b; Guillemot and Cepko, 1992; Park and Hollenberg, 1989; Pittack et al., 1991), the mechanism of retinal histogenesis remains largely unknown.

Because nuclear transcription factors function cell autonomously, they are good candidates for intrinsic regulators of retinal cell fate. Several classes of transcription factors are required for optic vesicle morphogenesis (Furukawa et al., 1997a; Mathers et al., 1997; Porter et al., 1997) and for differentiation of retinal cell types (Furukawa et al., 1997b). bHLH transcription factors regulate neurogenesis in both invertebrates and vertebrates (Jan and Jan, 1993; Lee, 1997; Kageyama et al., 1995). This class has been most extensively studied in the *Drosophila* nervous system; some family members act positively to promote neuronal cell development, whereas others antagonize the 'proneural' genes. The *Drosophila* proneural genes include the *achaete-scute* complex (*AC-S*, required for the development of external sense organs and subsets of CNS precursors), *atonal* (*ato*, necessary for chordotonal organ and photoreceptor development) and

daughterless (*da*, required for the formation of all embryonic central and peripheral nervous system neurons and photoreceptor cell development) (Campuzano and Modolell, 1992; Ghysen et al., 1993; Jarman et al., 1993, 1994; Caudy et al., 1988; Cronmiller et al., 1988; Brown et al., 1996). Conversely, bHLH proteins encoded by *extramacrochaete* (*emc*), *hairy (h)* and the *Enhancer of split* complex negatively regulate proneural gene function throughout the nervous system, by sequestering positive factors or repressing transcription directly (Van Doren et al., 1991, 1994; Ohsako et al., 1994).

Multiple vertebrate family members have been identified for each *Drosophila* bHLH subclass. Structurally, vertebrate proneural genes fall into two subsets, with one group, *Mash1, Mash2, Xash1* and *Xash3*, being more closely related to *Drosophila AC-S* genes (Ferreiro et al., 1992; Guillemot and Joyner, 1993; Johnson et al., 1990; Turner and Weintraub, 1994). The other, larger subset, which includes *Math1, Math2/Nex1, Math3/Xath3/NeuroM, Math4a/Ngn2, Math4b/Ngn3, Math4c/Ngn1, Xath5* and *NeuroD*, are more similar to *Drosophila ato* (Akazawa et al., 1995; Ben-Arie et al., 1996; Gradwohl et al., 1996; Kanekar et al., 1997; Lee et al., 1995; Ma et al., 1996; Roztocil et al., 1997; Shimizu et al., 1995; Sommer et al., 1996; Takebayashi et al., 1997). Within and between these classes, bHLH genes are often expressed in partially overlapping patterns throughout the developing CNS.

In the developing mammalian eye, *Mash1, Math3, Math4a/Ngn2* and *NeuroD* are expressed by retinal progenitor cells (Gradwohl et al., 1996; Guillemot and Joyner, 1993; Jasoni and Reh, 1996; Roztocil et al., 1997; Sommer et al., 1996; Takebayashi et al., 1997), although none appear to be expressed before RGC formation. The role of these genes during eye development is poorly understood. For example, *Mash1* is expressed by many retinal progenitors, but a targeted mutation in the *Mash1* gene produced no eye phenotype (Guillemot et al., 1993). However, explant culture of *Mash1*$^{-/-}$ mutant retinas demonstrated a delay in rod, horizontal and bipolar neuron differentiation (Tomita et al., 1996a). Bipolar cell number was decreased, while Müller glial cell number increased (Tomita et al., 1996a). These results suggest that *Mash1* regulates the formation of later born retinal neurons, especially bipolar cells, but has no role in early retinal neurogenesis. Instead, the formation of early-born retinal neurons in mammals may be regulated by *ato* family members, as in *Drosophila* photoreceptor cell development.

At least one negatively acting bHLH gene, *Hes1*, is required for mammalian eye development. *Hes1* is expressed during early stages of mouse eye development and is structurally related to *Drosophila h* and *Enhancer of split* genes (Sasai et al., 1992; Tomita et al., 1996b). Loss- and gain-of-function studies demonstrate that *Hes1* regulates the timing of retinal neurogenesis, as *Hes1*-deficient mouse embryos form severely reduced optic cups by embryonic day 10.5 (E10.5) (Tomita et al., 1996b). In the *Drosophila* eye, *h* (together with *emc*) influences the timing of *ato* expression (Brown et al., 1995). *Hes1* and *h* may have similar functions during retinal neurogenesis. Like *h*, *Hes1* may repress positively acting bHLH genes such as *Mash1*, which is prematurely upregulated in the optic cup and neural tube of E10.5 *Hes1*$^{-/-}$ embryos (Ishibashi et al., 1995). However, as yet no clear *ato* equivalent has been identified for mammalian retinogenesis that is subject to *Hes1* regulation.

The *Pax6* transcription factor is critically required for eye formation. It contains two highly conserved DNA-binding domains, a paired box and a homeobox (Hanson and van Heyningen, 1995). *Pax6* mutations produce eye malformations in the human disease aniridia (Glaser et al., 1992; Ton et al., 1991) and, in the mouse and rat, *Small eye (Sey)* traits (Fujiwara et al., 1994; Hill et al., 1991). *Sey*/+ heterozygotes have noticeably smaller eyes by midgestation (Hill et al., 1991; Hogan et al., 1986) and typically form cataracts postnatally. These malformations arise through haploinsufficiency in humans and in mice. A delay in lens induction has been postulated for *Sey*/+ heterozygotes (Theiler et al., 1978), but the basis for *Pax6* dosage sensitivity (Glaser et al., 1994) is unknown and no dosage-responsive downstream genes have been identified. Overexpression of human *Pax6* in mice has further demonstrated that *Pax6* gene dosage is critical for normal mammalian eye development (Schedl et al., 1996). *Sey/Sey* homozygotes initiate optic vesicle morphogenesis (Grindley et al., 1995), but fail to form lenses or complete retinal development. The resulting eyeless mice die at birth due to concomitant nasal and CNS defects (Grindley et al., 1995; Hill et al., 1991; Hogan et al., 1986). Because the primary eye defect in *Sey/Sey* embryos occurs prior to retinal neurogenesis, it has been difficult to understand if and how *Pax6* may regulate later eye formation events such as neuron specification.

Here we report a new murine bHLH gene, *Math5*, that is closely related to *Drosophila ato*. *Math5* retinal expression begins at E11, before any other mammalian proneural gene and is spatiotemporally correlated with the appearance of RGCs, the first-born neurons. To test whether *Math5* directly regulates this process, we compared the ability of *Math5*, *Mash1* and *Xath5* to promote differentiation of *Xenopus* retinal progenitors in vivo. Surprisingly, *Math5* and *Mash1* each bias retinoblast differentiation toward a bipolar cell fate, whereas *Xath5* promotes differentiation of RGCs. Finally, we show that *Pax6* is required for appropriate *Math5* and *Hes1* expression in the optic cup, thereby connecting Pax6 activity with retinal neuron formation.

MATERIALS AND METHODS

Molecular cloning of *Math5*

Reverse transcription was performed with random-primed mRNA from mouse E12.5 embryonic eye tissue and the resulting cDNA was used as a template for a degenerate polymerase chain reaction (PCR). Standard PCR conditions were used with an annealing temperature of 60°C for 40 cycles. The PCR primers corresponded to peptide sequences RRLAANA (5′-ARGRMGKCTRGCIGCMAAYGC-3′) and ETLQMAL (5′-GSGCCATCTGYAGIGTCTCRTA-3′), which are completely conserved within the bHLH domains of *Xenopus* Xath5 and *Drosophila* ato (Jarman et al., 1993; Kanekar et al., 1997). The resulting 135 bp PCR products were subcloned using a TA cloning kit (Invitrogen). Of nine plasmid subclones sequenced, six encoded Math5 bHLH domains and three encoded Math1 bHLH domains. The 135 bp *Math5* bHLH fragment was used as a probe to screen a mouse genomic DNA library in λEMBL3 (Satakato and Maas, 1994) and a P3-P7 mouse retinal cDNA library in λZap II. Five cDNA clones and a 2.8 kb *Hin*dIII fragment from one genomic clone were sequenced on both strands by automated DNA sequencing. DNA sequence

analysis was performed using MacVector and AssemblyLIGN programs, version 5.0 (Oxford Molecular Group). The GenBank accession number for *Math5* is AF071223.

Math5 and *Mash1* cDNAs were subcloned into the expression vector pCS2+ (Turner and Weintraub, 1994) at the *Eco*RI and *Xba*I sites (*Math5*) or the *Eco*RI site (*Mash1*). To create a C-terminal myc-epitope tag, the *Math5*-coding region was subcloned into the pCS2+MT expression vector following PCR amplification in the presence of MasterAmp PCR enhancer compound (Epicentre Technologies). The 5′ primer was 5′-TGCAGAGCGGCA-AGGCCT**ATG**AAGTCGGCCTGCAAACCC-3′ (*StuI* site underlined, ATG start codon in bold) and the 3′ primer was 5′-AACTCATTTCATCTAGATGTTTGAAACGGGAAGGAA-3′ (*Xba*I site underlined; 60 bp downstream of stop codon). Subclones generated by PCR were fully sequenced. Math5/pCS2+, Mash1/pCS2+ and Math5-MT/pCS2+ constructs produced proteins of the predicted size upon in vitro translation (TNT Coupled Reticulocyte Lysate System, Promega). No difference in functional activity was detected between pCS2-Math5 and the myc-epitope tagged version, Math5-MT/pCS2. Details of Xath5/pCS2+ constructs can be found in Kanekar et al. (1997).

Phylogenetic analysis

A total of 20 bHLH amino acid domain sequences, including Math5, were aligned by eye and subjected to parsimony analysis using PAUP, version 3.1.1 (Swofford, 1993). A heuristic search with 100 random stepwise addition replicates was performed using a step matrix for amino acid substitutions. This matrix gives the minimum number of nucleotide substitutions needed to convert one amino acid into another, based on the genetic code used by nuclear genes of most eukaryotes. 100 bootstrap replicates, each representing 100 random stepwise sequences of taxa addition (Swofford, 1993) were also performed and a bootstrap majority rule consensus tree was generated. In both searches, Mash1 and Mash2 bHLH domains were designated as outgroup taxa.

Chromosomal mapping

Mouse-hamster somatic cell hybrid DNAs (Lalley et al., 1978) were tested for *Math5* by PCR, using primers 5′-ACAGGGAGTGGTTTTATTCCTCCC-3′ (forward) and 5′-GTTGGTAGCTGGGCTTTGGAATCC-3′ (reverse), which amplify a 625 bp genomic DNA fragment located 800 bases 3′ from the *Math5* stop codon. Precise chromosome position was determined by linkage analysis of a PCR length variant between laboratory mice and *Mus spretus*. A set of 90 interspecific backcross progeny (Glaser et al., 1990) was typed using the *Math5* primer pair and microsatellite markers *D10Mit16*, *D10Mit109*, *D10Mit62*, *D10Mit42* and *D10Mit74*.

Mouse embryos

CD-1 embryos (Charles River) were obtained from timed matings. The day that vaginal plugs were observed was designated E0.5. Embryos were dissected in cold phosphate-buffered saline (PBS), their hindbrain and cerebral vesicles were incised and they were fixed overnight in 4% paraformaldehyde/PBS at 4°C. Embryos were kept in fixative for up to 2 weeks at 4°C, dehydrated stepwise through a graded PBS/methanol series and stored in methanol at –20°C. For some experiments, fixed E11.5-E13.5 embryos were bisected sagittally in methanol before processing for in situ hybridization.

Embryos from *Small eye* ($Sey^{Neu}/+ \times Sey^{Neu}/+$) heterozygous matings were isolated in cold PBS, fixed and processed for in situ hybridization. The genotype of each embryo was determined by PCR (Xu et al., 1997), using tail or extraembryonic membrane DNA (Laird et al., 1991) as a template. Littermates with identical or nearly identical (±1) somite numbers were utilized for analysis of *Math5* (4 litters) or *Hes1* (6 litters) mRNA expression. The Sey^{Neu} allele originated in a C3H × 101 F_1 mouse (Hill et al., 1991) and has been maintained on a C3H/HeJ background. To facilitate gene expression studies in the developing eye, the Sey^{Neu} mutation was backcrossed to the albino FVB strain for more than five generations. No difference was observed in eye morphology (E9.5 to E13.5), pattern of gene expression (*Math5* and *Hes1*) or *Sey* phenotype between these genetic backgrounds.

In situ hybridization and immunohistochemistry

Whole-mount in situ hybridization was performed on mouse embryos as described by Hargrave and Koopman (1998). Sense and antisense digoxigenin-labeled RNA probes were prepared from *Math5* cDNA clones in pBluescript II KS+, using a DIG RNA labeling kit (Boehringer Mannheim) and were detected by anti-digoxigenin antibody coupled to alkaline phosphatase. Hybridization and stringent posthybridization wash steps were performed at 70°C. After alkaline phosphatase development, embryos were destained for up to 4 hours in 1% Triton X-100/PBS, postfixed in 4% paraformaldehyde/PBS and photographed through a dissecting microscope using EPY 160T film and a dark-field condenser.

For in situ hybridization of tissue sections (Schaeren-Weimers and Gerfin-Moser, 1993), dissected embryos were immediately embedded and cryosectioned at 14 μm. The prehybridization, hybridization and stringent wash steps were performed at 70°C using the buffers described in Hargrave and Koopman (1998). Alkaline phosphatase color development was allowed to proceed for 24 hours. Slides were postfixed in 4% paraformaldehyde and mounted in 80% glycerol/PBS. Some sections were counterstained with Neutral Red (Sigma) prior to mounting. Mounted sections were digitally captured using an Optronics 3CCD Video Camera System or were photographed using EPY 64T film and scanned with a Nikon Coolscan slide scanner.

Mash1 (2 kb), *Hes1* (0.9 kb), *NeuroD* (1 kb) and *Ngn2* (1.5 kb) riboprobes were synthesized from cDNA plasmid clones. For double labels with *Math5* RNA and Pax6 protein, embryos or isolated eyes were processed for whole-mount in situ hybridization, embedded and cryosectioned at 14 μm. Sections were incubated with a rabbit polyclonal antisera reactive with the C-terminal peptide of the mouse Pax6 protein (Davis and Reed, 1996), processed and developed for peroxidase immunohistochemistry as described in Mastick et al. (1997). Double-labeled sections were mounted in 80% glycerol/PBS and digitally captured using a microscope equipped with Nomarski optics.

Microinjection of RNA into *Xenopus* embryos

Capped RNA was synthesized in vitro by SP6 transcription from Xath5/pCS2, Math5/pCS2, Math5-MT/pCS2, Mash1/pCS2, GFP/pCS2 or nuclear β-galactosidase (nβgal)/pCS2 template DNA using a Message Machine kit (Ambion). For 2-cell-stage injections, RNA was injected into one of the two blastomeres in the following amounts: Xath5 (500 pg), Math5 or Math5-MT (50-500 pg), nβgal (60 pg). Following injection, embryos were processed as described in Kanekar et al. (1997) with one exception: embryos injected with nβgal RNA were stained with magenta-gal (Biosynth International) using an X-gal staining method (Turner and Weintraub, 1994). The digoxigenin-labeled *Xenopus N-tubulin* riboprobe (Richter et al., 1988) was synthesized as previously described (Harland, 1991) and whole-mount in situ hybridization for *N-tubulin* mRNA was performed as detailed in Kanekar et al. (1997).

For 16-cell RNA injections, Math5 RNA (50-100 pg) was injected into *Xenopus* blastomere D.1.1. GFP RNA (50 pg) was coinjected to label cells derived from the injected blastomere. Following injection, the embryos were processed as described in Kanekar et al. (1997). Some sections of 16-cell-injected embryos were processed for NCAM immunohistochemistry using the 6F11 monoclonal antibody (Sakaguchi et al., 1989) and a rhodamine-conjugated goat anti-mouse IgG secondary antibody (Jackson Immunoresearch).

In vivo lipofection and BrDU analysis

In vivo lipofection of experimental and green fluorescent protein (GFP) DNA (to mark transfected cells) was performed and analyzed as previously described (Kanekar et al., 1997). The rate of cotransfection of two plasmids is very high (Holt et al., 1990). Images of labeled sections (lipofections and 16-cell RNA injections) were digitally captured by a Xillix Microimager PMI CCD camera using Openlab software. Lipofected embryos were injected with 5 mg/ml BrDU at stage 26-27 as described in Wetts et al. (1993), then fixed and processed at stage 41. The embryos were cryostat-sectioned and digital images of GFP-labeled retinal sections captured as described above. BrDU labeling in these sections was then detected by immunocytochemistry (del Rio and Soriano, 1989) using a monoclonal anti-BrDU antibody (Sigma) and the rhodamine-conjugated goat anti-mouse secondary antibody described above. Images of the anti-BrDU-stained retinal sections were then acquired digitally and merged with the GFP images from the same sections to determine which cells are both GFP positive and BrDU positive.

RESULTS

Isolation and structural analysis of *Math5*

To investigate how bHLH genes regulate early retinal neurogenesis, we screened embryonic mouse eye cDNA (E12.5) for new *ato*-related transcription factors by degenerate RT-PCR. Primers that amplify the conserved bHLH domain were designed based upon segments of significant amino acid identity between *Drosophila* ato and *Xenopus* Xath5 (Jarman et al., 1993; Kanekar et al., 1997). The resulting 135 bp products were cloned and sequenced. Two classes of clones were identified by sequence and colony hybridization: *Math1* (Akazawa et al., 1995) and a novel sequence most closely related to *Xath5*, which we have termed *Math5*. The *Math5* bHLH fragment was used to probe mouse genomic and P3-P7 eye cDNA libraries. Four different cDNA clones were obtained ranging in length from 1.2 kb to 1.4 kb. All of the clones contain an identical 447 nucleotide open reading frame encoding a protein of 149 amino acids (Fig. 1A). The putative methionine start site conforms to the Kozak consensus sequence (Kozak, 1989) and is preceded by stop codons in all three frames. A 17 kb genomic clone was also isolated. The genomic and cDNA sequences are identical, indicating that *Math5* contains an intronless open reading frame (Fig. 1A).

Aligned Math5 and Xath5 proteins are 91% identical within the bHLH domain (Fig. 1A,B) and exhibit limited stretches of identity outside of this domain (Fig. 1A). A phylogenetic comparison of Math5 bHLH amino acid sequence with other bHLH proteins was also performed. A heuristic search generated a consensus phylogram based on shared, derived characteristics with Mash1 and Mash2 as outgroup taxa. Bootstrap analysis also strongly supported this phylogram (Fig. 1C). In the heuristic search, 28 most parsimonious trees were produced. The length of the shortest tree is 239 steps. A strict consensus of these 28 trees, as well as the bootstrap majority rule consensus tree (Fig. 1C) demonstrate that Math5 is a derived member of the ato protein family and is most closely related to Xath5. In addition, Math5 is as closely related to *Drosophila* ato as it is to the lineage giving rise to Math1, Hath1 and Cath1. Finally, this analysis indicates that the *C. elegans* lin32 protein is a member of the ato family and does not belong to the AC-S family (Fig. 1C).

Chromosome mapping of *Math5*

Math5 was mapped using a mouse-hamster somatic cell hybrid panel (Lalley et al., 1978) and an interspecific mouse backcross (Glaser et al., 1990). In the somatic hybrids, *Math5* segregated discordantly with every chromosome except 10. In the interspecific backcross, *Math5* was further localized to a region approximately 34 cM from the centromere (Fig. 1D). No recombination was observed between *Math5* and *D10Mit62* among 90 N_2 progeny (Fig. 1D). This position excludes a role for *Math5* in the *eye blebs* mutation or in any of several dominant cataract mutations (*Cat, Cat3, Cat5*) on chromosome 10 (Loster et al., 1997). No human genetic eye diseases were found to map within the regions syntenic to this portion of mouse chromosome 10 (N. L. B., unpublished data). *Math3 (Atoh3)*, another *ato*-like gene expressed in the developing mouse eye, also maps to chromosome 10 (Isaka et al., 1996). However, *Math3* and *Math5* are at least 40 cM apart and so do not represent a gene cluster for the bHLH protein family.

Expression of *Math5* during eye development

The spatial and temporal expression of *Math5* mRNA was examined during mouse embryonic development by whole-mount and sectioned in situ hybridization. *Math5* was first detected at E11 (Fig. 2A-D), in a small patch of cells in the central, dorsal optic cup (Fig. 2B). From E11 to E12, the dorsal expression domain expands circumferentially (Fig. 2C). By E12.5, *Math5*-expressing cells are distributed throughout the developing retina (Fig. 2F,I), except for the ciliary proliferating zone (Fig. 2E,J). These cells are arranged in columnar strings or clusters, interspersed with columns of nonexpressing cells (Fig. 2D,F-H).

As retinal neurons differentiate, they exit the cell cycle and migrate toward the inner (vitreal) side of the optic cup to assume their final position (Young, 1983, 1985). Progenitor cells remain in the outer (ventricular) side. Accordingly, the retina ceases to be a uniform sheet of neuroepithelial cells. Cell division is primarily restricted to the ventricular zone and the ciliary margin of the optic cup. During later stages of development (≥E13.5) a single *Math5*-positive cell was often observed adjacent to the ciliary proliferating zone (arrow in Fig. 2E) and in columns of cells toward the central retina (arrowheads in Fig. 2E). The first neurons to differentiate are RGCs, which appear at the late E12.5/early E13 stage of development as shown by birthdating and terminal differentiation marker studies (Erkman et al., 1996; Hinds and Hinds, 1974). *Math5* expression begins a full day prior to this time. Differentiated RGCs, clearly visible within a central domain and marked by their strong expression of Pax6 protein, do not express *Math5* (Fig. 2J,K). The period of *Math5* expression thus precedes and overlaps retinal neurogenesis. Although *Math5* was detected in retinal progenitor cells from E11 through birth (Figs 2L, 4I), the number of positive cells decreased significantly at E16.5 (Fig. 4A). At birth (P0), *Math5*-expressing cells were primarily observed adjacent to the ciliary margin and sparsely distributed within the central retina (Figs 2L, 4I). No *Math5* expression was detected in the adult retina (data not shown).

Math5 expression in other embryonic tissues

In addition to the eye, we observed *Math5* expression only in the developing tenth cranial (vagal) ganglion between E13.5

and E15.5 (Fig. 2M). This contrasts with *Xath5*, which is found in the developing frog retina, nasal placodes and pineal gland (Kanekar et al., 1997) and with *ato*, which is expressed in the developing *Drosophila* eye, olfactory system and ocellus, a photosensitive structure that has been likened to the pineal gland (Jarman et al., 1995; Reddy et al., 1997). We were unable to detect *Math5* expression, from E8.5 to birth, in the murine nasal placode, olfactory epithelium or developing pineal gland. At the same time, a comparable probe, *Mash1*, was easily detected in the nasal placode and olfactory epithelium (data not shown). Although *Xath5* is not expressed by cells of the *Xenopus* vagal ganglion (M. L. V., unpublished observations), other mammalian *ato*-related family members, such as *ngn2*, are expressed in particular cranial ganglia prior to neuron formation (Ma et al., 1998).

Math5 and *Hes1* retinal expression require Pax6 function in a dose-dependent manner

The *Pax6* gene is expressed throughout vertebrate eye development and controls many aspects of ocular formation. *Pax6* expression begins at mouse E8.0 within the neural plate and optic vesicle and persists throughout eye development into adulthood (Koroma et al., 1997; Walther and Gruss, 1991). Early *Pax6* expression is ubiquitous within the optic cup (Walther and Gruss, 1991) while later it becomes restricted to differentiating RGCs and amacrine cells (Belecky-Adams et al., 1997). To test whether *Pax6* function regulates *Math5* transcription, we examined *Math5* mRNA expression in *Sey*/+ × *Sey*/+ litters at E11.5. Optic vesicle development in *Sey/Sey* embryos arrests at the E9.5 stage of morphogenesis but optic vesicle and stalk structures are present at E11.5 (Grindley et al., 1995). We saw no expression of *Math5* in *Sey/Sey* embryos (Fig. 3C,F), even at the earliest time of *Math5* expression, the 46 somite (E11) stage (data not shown). We consistently observed a marked reduction in the size of the *Math5* expression domain in *Sey*/+ embryos (compare Fig. 3B to A and E to D), strongly suggesting that *Math5* expression depends upon *Pax6* function. As yet, no other downstream targets of *Pax6* regulation are known to display a similar gene dosage dependence.

The mouse bHLH gene *Hes1* is

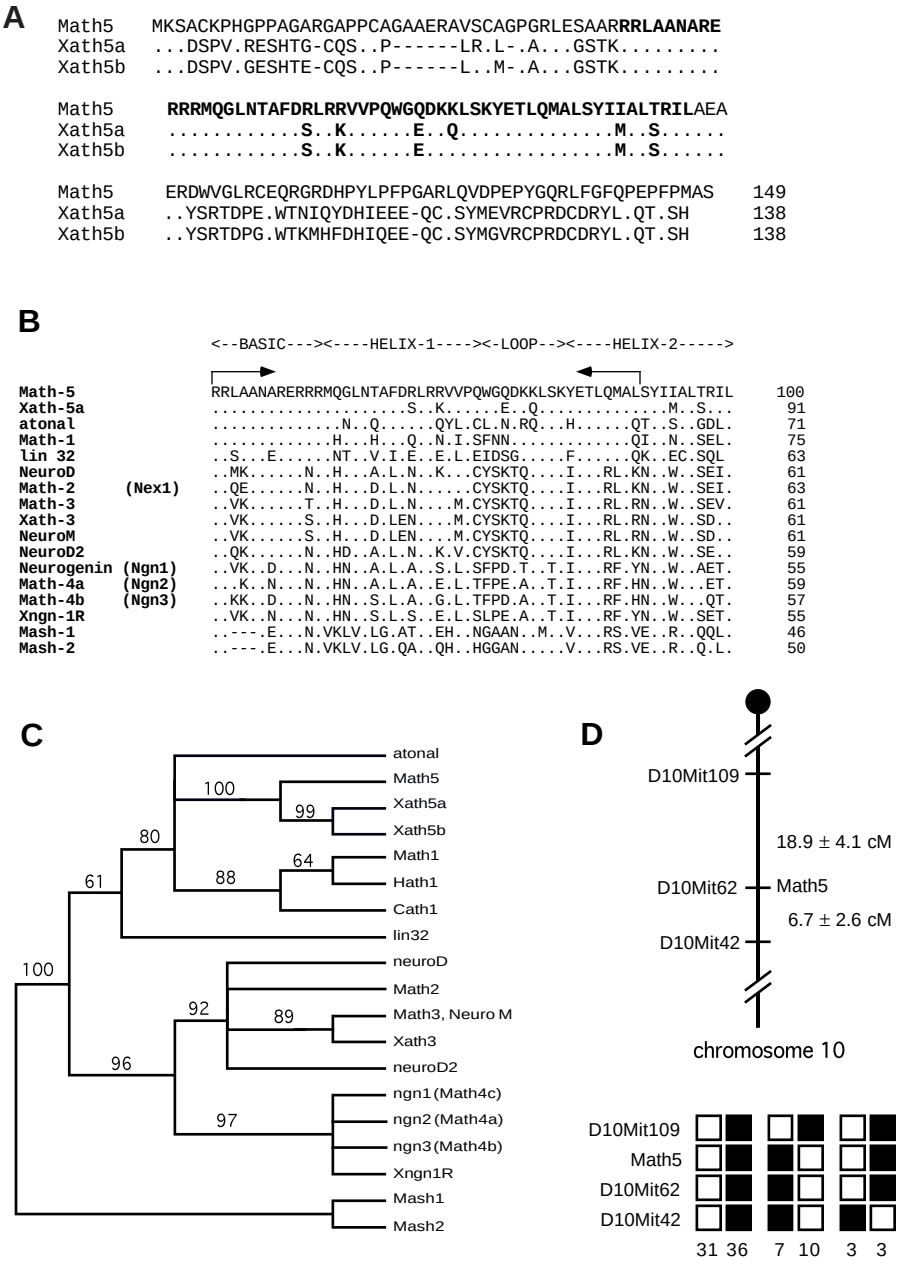

Fig. 1. Math5 protein sequence, phylogenetic analysis and genetic mapping. (A) Complete peptide sequence of Math5 aligned to Xath5a and b (Kanekar et al., 1997). Due to partial duplication of the *Xenopus* genome, two Xath5 proteins have been identified (Kanekar et al., 1997). Within the bHLH domain, there is an additional amino acid identity when Math5 is compared to Xath5b alone. Dots indicate amino acid identity and dashes represent gaps for optimal alignment. The bHLH domain is delineated by bold typeface. (B) Comparison of bHLH domains (56 residues). Basic, helix and loop regions are indicated above the aligned sequences, along with the position of degenerate PCR primers (arrows). The percent amino acid identity to Math5 is at the right. (C) A bootstrap majority rule consensus tree of the ato family obtained by comparing 20 bHLH domains (56 characters). bHLH domain peptide sequences were used in a single parsimony analysis, with Mash1 and Mash2 as outgroup taxa. Numbers on the branches indicate percentage of bootstrap replications that support the group descending from each node. A value over 70 indicates very strong support. The strict consensus tree from our heuristic analysis is identical with the exception that Math3 and Xath3 are unresolved. (D) Chromosomal mapping of *Math5*. (Top) Partial linkage map indicating the location of *Math5* in relation to microsatellite markers, with recombination frequencies (±standard error) in centimorgans (cM). (Bottom) Recombination data obtained from 90 interspecies backcross progeny. (■, *M. spretus* progeny; □, laboratory mouse; allele transmitted by the N_1 parent).

expressed in the optic cup at E11.5 and functions in retinal formation (Tomita et al., 1996b). To explore the relationship between *Hes1*, *Pax6* and *Math5*, we examined *Hes1* expression in *Sey/+* × *Sey/+* litters at the identical somite ages as for *Math5* (Fig. 3G-L). In these experiments, *Hes1* expression also depended upon *Pax6* gene dosage, but in an reciprocal manner to *Math5*. *Hes1* mRNA expression was increased in *Sey/+* embryos in comparison to wild-type (compare Fig. 3H to G and K to J), and was abundant within the optic vesicle remnant of *Sey/Sey* embryos at E11.5 (Fig. 3I,L). *Pax6* function is similarly required for proper *Hes1* expression at E10.5, when the increase in *Hes1* expression in *Sey/Sey* optic vesicles is more striking (Fig. 3M-O). The size of the *Hes1* expression domain in E10.5 *Sey/Sey* optic vesicles reflects abnormal morphology of this structure (Grindley et al., 1995) rather than an increased number of cells expressing *Hes1* (N. L. B., unpublished observations). These findings suggest that *Pax6* may negatively regulate *Hes1* expression. The effects of *Pax6* deficiency upon *Hes1* are eye-specific, since no changes in *Hes1* mRNA were noted in other expression domains such as the tailbud, somites and spinal cord (data not shown). We conclude that *Pax6* function is required to properly regulate the expression of *Math5* and *Hes1* in the developing optic cup.

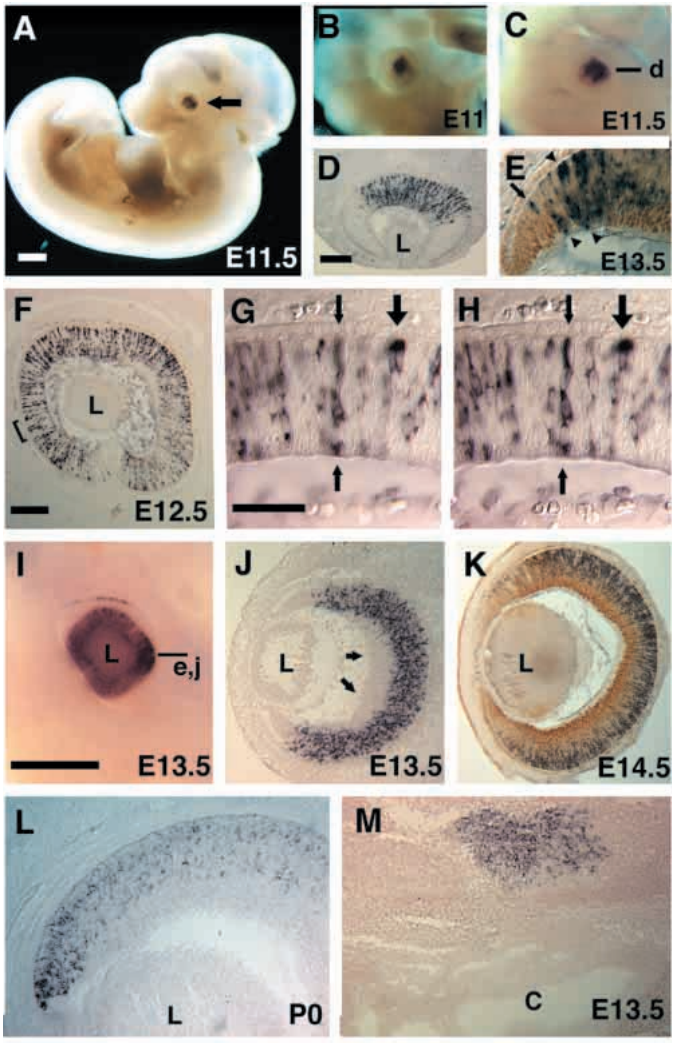

Math5 precedes *NeuroD, Ngn2 and Mash1* in the developing retina

Several studies of vertebrate proneural genes have suggested a hierarchy of regulatory relationships within the bHLH family (Cau et al., 1997; Kanekar et al., 1997). For example, during mammalian olfactory neurogenesis, *Mash1* activates a bHLH gene cascade within neural progenitor cells (Cau et al., 1997). In this study the *AC-S*-related gene *Mash1* was shown to precede and act upon *ato*-like genes. To evaluate this relationship in the murine eye, we compared the spatial and temporal expression of *Math5* to that of *Mash1*, the only known *AC-S* family member expressed in the mammalian retina (Guillemot and Joyner, 1993; Jasoni and Reh, 1996), and to *NeuroD* and *Ngn2*, *ato*-like genes with retinal expression (Gradwohl et al., 1996; Lee et al., 1995; Sommer et al., 1996).

Math5 expression initiates at E11 in the central optic cup (Fig. 2B) and *Ngn2* and *NeuroD* mRNA are not detected at this time (data not shown). Instead, *NeuroD* and *Ngn2* initiate expression at E13.5 (Fig. 4B-D), 2 days after *Math5* (Figs 2I,J, 3A). Interestingly, *NeuroD* is expressed in two domains at all ages examined (Fig. 4B,C,F,J), within the outermost cells of the ventricular zone and differentiated RGCs. This suggests *NeuroD* may function in progenitors as well as in terminally differentiated neurons. *Mash1* retinal expression initiates at E14.5 (Guillemot and Joyner, 1993; Jasoni and Reh, 1996), 3

Fig. 2. *Math5* expression during embryogenesis. In situ hybridization of whole-mount (A-I,K) and sectioned (J,L-M) embryos with *Math5* digoxigenin-labeled riboprobes. Rostral is at the left in B-F, I, M and at the top in G,H,J-L. (A-C) Lateral views of E11-11.5 embryos showing *Math5* expression exclusively in the optic cup (arrow in A). *Math5* optic cup expression begins at E11 (46-somite stage) in a dorsal patch of cells. This domain expands throughout the next 24 hours to encompass the entire optic cup. (D) Horizontal section of E11.5 optic cup, as indicated in C. *Math5*-expressing cells span the retinal epithelium and are interspersed with groups of nonexpressing cells. (E) Horizontal section of an E13.5 retina, oriented as indicated in I, labeled for *Math5* mRNA (blue cells) and Pax6 protein (brown nuclei), and viewed at high magnification. Undifferentiated cells at the ciliary margin (lower left) and differentiated RGCs (lower right) express Pax6. An isolated *Math5*-expressing cell (arrow) is adjacent to the undifferentiated region. Toward the central retina (right), columnar clusters of *Math5*-expressing cells (arrowheads) are separated by columns of nonexpressing cells. (F-H) Sagittal section of E12.5 optic cup showing the interspersion of *Math5*-positive and -negative cells. (G-H) High magnification views of the area marked by a bracket in F, at two different focal planes. Two strongly *Math5*-positive cells at the ventricular surface of the neuroretina (large arrow) appear to have recently divided. The columnar arrangement of *Math5*-positive cells, spanning the width of the optic cup, is indicated (small arrows). (I) Lateral view of an E13.5 eye showing strong *Math5* expression throughout the retina. (J) In situ hybridization at E13.5, sectioned as indicated in I and counterstained with neutral red. Differentiated RGCs (arrows) do not express *Math5* (blue cells). (K) Transverse section of E14.5 eye labeled for *Math5* mRNA (blue cells) and Pax6 protein (brown nuclei). Pax6 protein is abundant in RGCs, located on the vitreal side of the retina, while undifferentiated cells in the ventricular zone are *Math5*-positive. (L) At birth, *Math5* expression is restricted to the undifferentiated region of the retina, closest to the ciliary margin (lower left). (M) Vagal (tenth) cranial ganglion cells express *Math5* (blue cells) at E13.5 (counterstained with neutral red). Scale bars 500 μm in A-C, I; 100 μm in F, J-M; and 50 μm in D, E,G,H. Abbreviations: L, lens; c, cochlea.

days after the onset of *Math5*. All four genes are strongly expressed by retinal progenitors from E14.5 to E16.5, as judged by in situ hybridization to sections of embryonic eyes (Fig. 2K and Gradwohl et al., 1996; Sommer et al., 1996).

At E16.5 the number of *Math5*- and *Ngn2*-expressing cells begins to noticeably diminish (Fig. 4E,H), whereas *Mash1* is expressed by most, if not all, progenitors (Fig. 4G). In similar whole-mount experiments, Jasoni and Reh (1996) observed that *Mash1* is expressed by 10-30% of the progenitor population at a given time. By birth, *Math5* and *Ngn2* expression are nearly absent from the central retina (Fig. 4I,L), while *Mash1* and *NeuroD* expression are widespread (Fig. 4J,K). *Mash1* expression persists until postnatal day 9 (Jasoni and Reh, 1996) and *NeuroD* mRNA is present in the adult retina (Acharya et al., 1997). Birthdating studies have shown that retinal histogenesis can be divided into an early phase (from E10.5 to birth), when most RGCs, cones and horizontal cells are born, and a later phase (from E15 to postnatal day 9) when the majority of bipolar, amacrine, rod and Müller glial cells are generated (Carter-Dawson and LaVail, 1979; Young, 1985). Our findings correlate *Math5* and *Ngn2* expression with the appearance of early-born neurons, *Mash1* expression with late phase neurogenesis and *NeuroD* expression with both phases of retinal neuron formation.

Math5 promotes ectopic neurogenesis and retinal expansion in *Xenopus* embryos

Since Math5 and Xath5 share a high degree of sequence identity within the bHLH domain, we tested whether they have similar functional activity. Xath5, like other ato-related bHLH proteins, is able to promote the formation of ectopic *N-tubulin*-positive cells when overexpressed in *Xenopus* embryos by 2-cell RNA injection (Kanekar et al., 1997). We therefore injected *Math5* RNA into one cell of a 2-cell-stage embryo, collected the embryos at the open neural plate stage and probed by whole-mount in situ hybridization for *N-tubulin* expression, a neuron-specific marker (Richter et al., 1988). Coinjected nβ*gal* RNA was detected by staining with magenta-gal, which marked the injected side of the embryo (Fig. 5Ai). Overexpression of *Math5* caused the appearance of ectopic *N-tubulin*-positive cells throughout the neural plate and lateral ectoderm on the injected side with a very punctate pattern of staining similar to what is seen with overexpression of Xath5 (30/30 embryos, Fig. 5Aii) (Kanekar et al., 1997). This suggests that *Math5* can promote neuronal differentiation when overexpressed.

Targeted expression of *Xath5* in retinal progenitor cells using both 16-cell RNA injection and in vivo lipofection caused a strong bias toward the RGC fate (Kanekar et al., 1997 and Fig.

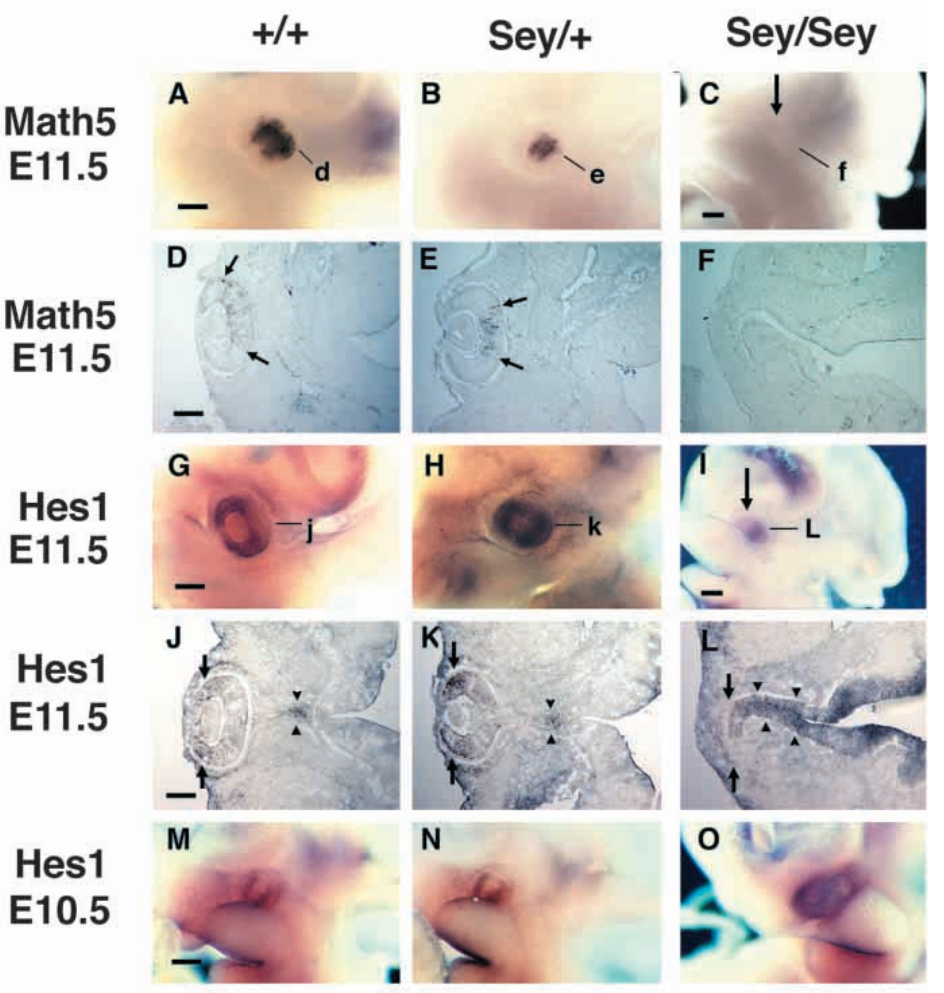

Fig. 3. Retinal expression of *Math5* and *Hes1* requires *Pax6*. Whole-mount in situ hybridization of matched 52-somite E11.5 (A-L) and 36-somite E10.5 (M-O) embryos from *Sey*/+ × *Sey*/+ litters. In A-C, G-I and M-O, embryos are oriented with rostral at the left and dorsal at the top. *Math5* mRNA is expressed in the central, proximal portion of the forming retina (A-F), whereas *Hes1* mRNA is present in the peripheral, distal optic cup (G-O). (A-F) *Math5* expression in E11.5 littermates. Lines in A-C indicate the plane of section shown in D-F. The number of *Math5*-expressing cells and the width of the expression domain (arrows in D and E) are greatly reduced in *Sey*/+ embryonic eyes, and absent in *Sey/Sey* optic rudiments (arrow in C). (G-L) *Hes1* expression in the optic cups of E11.5 littermates. Lines in G-I indicate the plane of section shown in J-L. The *Sey*/+ optic cup contains more *Hes1* mRNA in comparison to wild-type (arrows in J,K). *Hes1* is expressed in the optic vesicles of *Sey/Sey* mutant embryos (arrow in I), although the most distal cells of the optic vesicle do not express *Hes1* (arrows in L). In J-L, normal expression of *Hes1* in the optic stalk is unaltered in *Sey*/+ embryos, but greatly increased and in *Sey/Sey* embryos (arrowheads in J-L). (M-O) At E10.5 *Hes1* mRNA is already upregulated in *Sey/Sey* optic vesicles (O). No difference in *Hes1* expression was observed between wild-type and *Sey*/+ embryos at this age (compare M to N). Scale bars 300 μm in A,B,G,H,M-O; 500 μm C,I; 100 μm in D-F,J-L.

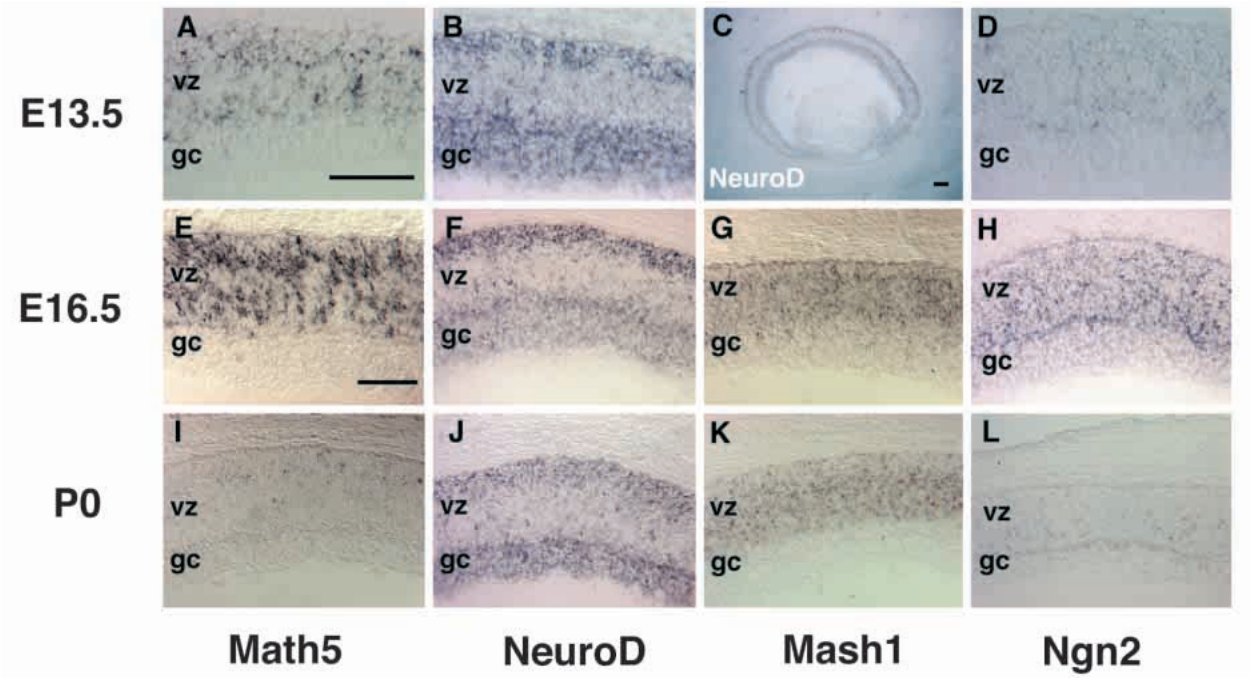

Fig. 4. Comparison of retinal bHLH gene expression during mouse eye development. In situ hybridization of adjacent sections with digoxigenin-labeled RNA probes for *Math5* (A,E,I), *NeuroD* (B,C,F,J), *Mash1* (G,K) and *Ngn2* (D,H,L) at E13.5 (A-D), E16.5 (E-H) and birth (P0) (I-L). *Math5* (A), *NeuroD* (B,C) and *Ngn2* (D) mRNA are all present at E13.5 in the developing mouse retina, but *Math5* and *NeuroD* are more highly expressed than *Ngn2*. *NeuroD* is expressed in both the outer ventricular zone and the differentiating ganglion cell layer while *Math5* is restricted to the ventricular zone (compare Figs 3C to 2J). At E16.5, both *Math5* and *Ngn2* are expressed by subsets of cells in the ventricular zone (E,H), but *Mash1* is more generally expressed by retinal progenitors (G) and *NeuroD* (F) expression continues in two layers. In the newborn retina (P0), *Math5* and *Ngn2* expression are both greatly reduced to only a few progenitor cells (I,L) but *NeuroD* (J) and *Mash1* (K) are strongly expressed as at E16.5. vz, ventricular zone; gc, ganglion cell layer. Scale bar 50 μm.

6). To determine whether *Math5* has an effect on progenitor cell formation, *Math5* expression was targeted to the developing retina by injecting a mixture of *Math5* and GFP RNA into blastomere D.1.1 of 16-cell *Xenopus* embryos. This blastomere contributes to over 50% of the cells in the ipsilateral retina (Huang and Moody, 1993; Moody, 1987). The GFP signal was then used to identify clones of cells derived from the injected blastomere in sections of stage 41 embryos. In control embryos injected with GFP RNA alone, clusters of GFP-positive retinal cells spanned the neural and pigmented cell layers (n=17 retinae, Fig. 5Bii). Embryos co-injected with *Math5* and GFP RNA also contained clusters of GFP-positive cells within the retina (Fig. 5Bv) but the cell layers were severely disrupted within these clusters (n=17/19 retinae, Fig. 5Biv). This marked disruption in retinal structure suggested a block in the differentiation of cells overexpressing *Math5*.

We therefore stained the sections with antibodies against NCAM to determine whether the labeled cells had any features of differentiated neurons. We found that clones of GFP-positive cells in *Math5*-overexpressing embryos (Fig. 5Bvi) were weakly NCAM-positive, indicating that these cells showed some evidence of neuronal differentiation. We also observed a continuous population of GFP-positive cells extending from the back of the retina to the neural tube and, in some cases, relatively large clones of GFP-positive clones were also identifiable within the neural tube (data not shown). This might indicate either hyperplasia of neural retinal cells expressing *Math5* causing expansion towards the neural tube, or a failure of the evaginating optic cup to resolve from the neural tube when *Math5* is overexpressed. This expanded retinal phenotype and disruption of retinal organization was never observed when *Xath5* was overexpressed by 16-cell RNA injection (Kanekar et al., 1997). This suggests that not all aspects of *Xath5* function are conserved in *Math5*.

In vivo lipofection of *Math5* and *Mash1* promotes retinal bipolar cell fates

Because 16-cell injection of *Math5* and *Xath5* RNA had different effects, we used in vivo lipofection to further analyze their functional activities in *Xenopus* retinal progenitors. Stage 18 embryonic optic vesicles were injected with GFP DNA, alone or in combination with *Xath5, Math5* or *Mash1* DNA, accompanied by a lipid transfection reagent (Holt et al., 1990). The transfected GFP-positive cells were scored by morphology at stage 41 in retinal sections. In most cases, GFP fluorescence in transfected cells allowed unambiguous identification of retinal cell type based upon laminar position and morphology (Holt et al., 1990; Kanekar et al., 1997).

In a previous study (Kanekar et al., 1997), in vivo lipofection of *Xath5* and GFP DNA was shown to cause a dramatic bias towards the RGC fate (Fig. 6B,D), compared with control lipofection of GFP DNA alone (Fig. 6A,D). Increased representation of early-born RGCs caused by *Xath5* overexpression was at the expense of later-born cell types such as amacrine, bipolar and Müller glial cells. In contrast, in vivo lipofection of *Math5* and GFP DNA produced a dramatic

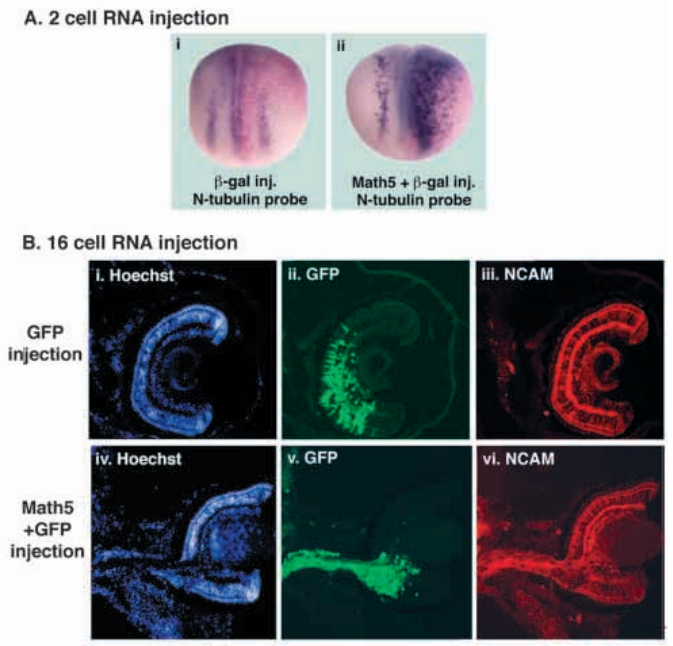

Fig. 5. Overexpression of *Math5* in *Xenopus* embryos by RNA injection. (A) Injection into one cell of a 2-cell Xenopus embryo with RNA for nβgal alone (i) or in combination with Math5 (ii). Stage 14-15 embryos were stained to detect β-galactosidase activity (magenta) and probed by whole-mount in situ hybridization for N-tubulin expression (purple). Embryos are oriented in a dorsal view with anterior at the top and injected side on the right. (i) Control embryo expressing nβgal alone demonstrating the normal pattern of *N-tubulin* expression in the neural plate. (ii) Embryo expressing both *Math5* and nβgal with ectopic *N-tubulin* on the injected side. (B) Injection into blastomere D.1.1 of a 16-cell Xenopus embryo with RNA for GFP alone (i-iii) or with RNA for *Math5* plus GFP (iv-vi). The embryos were fixed and cryostat sectioned at stage 41. Sections were immunostained for NCAM and labeled with Hoechst to visualize the retinal cell layers. (i-iii) Retinal section from a control embryo injected with GFP RNA alone. Hoechst staining reveals normal lamination (i). Within the retina, a large cluster of cells derived from the injected blastomere is labeled by GFP (ii) and robust NCAM staining is observed (iii). (iv-vi) A retinal section from an embryo injected with GFP and *Math5* RNAs. Hoechst staining highlights a disruption in the normal arrangement of retinal cell layers (iv). This disrupted region corresponds to a cluster of GFP-labeled cells within the retina (v). The GFP-positive cells, including those extruding from the back of the retina, are NCAM-positive (vi). Scale bar 1 μm.

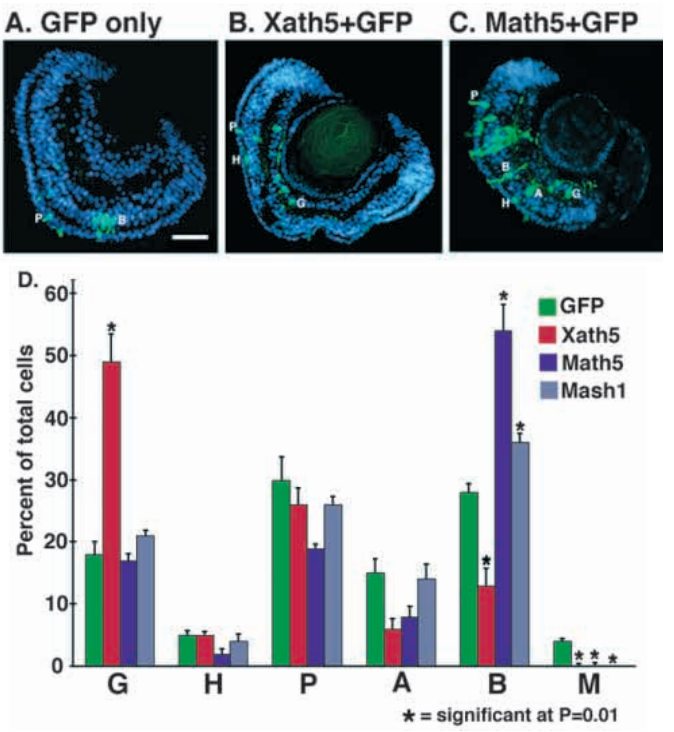

Fig. 6. In vivo lipofection of *Math5* promotes retinal bipolar cell fates. Embryos were transfected at stage 18 in the region of the optic vesicle with DNA for GFP alone (A) or GFP in combination with *Xath5* (B), *Math5* (C) or *Mash1* (not shown). At stage 41 these embryos were fixed, cryosectioned and stained with Hoechst dye to visualize the retinal cell layers. GFP-labeled cells were scored in retinal sections by laminar position and morphology. In section of embryos transfected with *Xath5*, there are more labeled cells in the RGC layer (B), while sections of embryos transfected with *Math5* show both a larger number of GFP-labeled cells overall and more labeled bipolar cells (C). Bipolar cells were scored as cells with distinct cell bodies in the INL and with thin processes extending radially but not extending into the ONL or GCL. These can be distinguished from Müller glial cells, which are radially oriented but have a more complex morphology (see Dorsky et al, 1995). (D) Percentage of retinal cell types labeled following transfection with DNA for GFP (green, *n*=432 cells from 5 eyes), GFP plus *Xath5* (red, *n*=939 cells from 5 eyes), *Math5* (navy, *n*=866 cells from 7 eyes) or *Mash1* (light blue, *n*=440 cells from 6 eyes). *Xath5* data are derived from Kanekar et al. (1997) and are included here for comparison. Expression of *Xath5* biases progenitors toward RGC fate, while both *Math5* and *Mash1* promote the formation of bipolar cells. The per cent representation of each cell type was calculated as a weighted average. Error bars indicate SEM; asterisk, $P<0.01$ by Student's t-test. Cell types on the graph are listed from left to right in rough order of birth. Abbreviations: G, retinal ganglion cell; B, bipolar cell; P, photoreceptor; A, amacrine cell; H, horizontal cell. Scale bar 0.5 μm.

increase in bipolar cells, one of the last neuronal cell types to be born in the retina (Fig. 6C,D). However, both *Xath5* and *Math5* overexpression suppressed Müller glial cell differentiation (Fig. 6D). We also noted larger clusters of labeled cells in retinae transfected with *Math5* as compared with *Xath5* or GFP alone (data not shown), suggesting that *Math5* might delay the differentiation of retinal progenitor cells and allow them to continue to proliferate. This property would be consistent with the observed bias toward late-born retinal cell types. To test this, we labeled embryos with BrDU soon after lipofection then collected the embryos at stage 41 and scored the number of transfected cells that were BrDU positive. We found that a similar percentage of transfected cells were BrDU-positive for both Math5 (49%, *n*=83 cells) and control embryos (47%, *n*=79 cells) arguing against a specific effect on proliferation of retinal precursor cells. As a control, the function of a second mammalian retinal bHLH gene, *Mash1* was tested in this assay. In vivo lipofection of *Mash1* DNA caused a significant bias toward bipolar cell fate although less dramatically than *Math5* overexpression (Fig. 6D). This result is consistent with an observed delay in mammalian bipolar cell development in the absence of *Mash1* (Tomita et al., 1996a).

DISCUSSION

We have characterized a new mouse bHLH gene, *Math5*, that is closely related to *Xenopus Xath5* and *Drosophila ato*. *Math5* is expressed in the developing optic cup, from E11 through birth and in the tenth cranial ganglion. In the retina, *Math5* expression precedes the differentiation of all neurons and is closely associated with RGC birthdates. When ectopically expressed in *Xenopus* embryos, *Math5* exhibits proneural activity and can alter retinal cell fates. We have also demonstrated that, in the developing mouse optic cup, *Math5* and *Hes1* are reciprocally regulated by *Pax6*.

Math5 and *Hes1* are targets of *Pax6* regulation

Pax6 has been proposed to act at or near the top of a regulatory hierarchy of transcription factors controlling invertebrate and vertebrate eye formation (Desplan, 1997; Halder et al., 1995). However, very few *Pax6* target genes have been identified during vertebrate eye development (Cvekl and Piatigorsky, 1996; Xu et al., 1997). We have identified two murine bHLH transcription factors, *Math5* and *Hes1*, whose expression relies upon *Pax6*. Interestingly, both genes require *Pax6* in a dose-dependent manner, but we do not yet know whether *Math5* and/or *Hes1* are direct transcriptional targets. Their strict dependence upon *Pax6* gene dosage suggests that this may be the case and provides a molecular entry point for understanding the haploinsufficiency of *Pax6* ocular phenotypes.

Remarkably, *Pax6* deficiency in mice affects *Math5* and *Hes1* opposite directions. *Math5* expression is downregulated and *Hes1* expression is upregulated in the absence of *Pax6* (Fig. 3). There are two possible mechanisms for such regulation, which are not mutually exclusive. *Pax6* may independently regulate *Hes1* and *Math5*, or it may do so in a linear, sequential manner. In the latter case, *Pax6* represses *Hes1*, which represses *Math5*. We favor the second possibility because changes in *Pax6* gene dosage affect *Math5* and *Hes1* expression differently (Fig. 3). Decreases in *Pax6* expression increase *Hes1* mRNA levels (Fig. 3G-L) but lower the number of *Math5*-expressing cells (Fig. 3A-F). *Pax6* may directly regulate *Hes1* transcription. In turn, *Hes1* would regulate *Math5* expression thereby influencing the timing or extent of retinal neurogenesis. This pathway can be further tested by examining *Math5* expression in *Hes1* mutant embryos and analyzing *Math5* and *Hes1* genomic DNA for the presence of eye enhancers with Hes1- or Pax6-binding sites.

Our proposed pathway is consistent with the proneural activity of *Math5* (Fig. 5B), the relative timing of *Hes1* and *Math5* expression in the optic cup and observations involving related genes. *Hes1* represses *Mash1* in the developing mouse eye and nervous system (Ishibashi et al., 1995), and *h* represses *AC-S* proneural genes in the *Drosophila* nervous system (Ohsako et al., 1994; Van Doren et al., 1994). In addition, *h* and *emc* are required for proper *ato* expression in the developing fly eye (Brown et al., 1995). Interestingly, the expression of *h* and *ato* appear to overlap with *Pax6 (eyeless)* (Brown et al., 1995; Halder et al., 1998). Whether *ato* and *h* are *eyeless* target genes and can be integrated into the network of early eye genes remains to be determined. Finally, a similar pathway has emerged for sensory nerve cell determination in *Caenorhabditis elegans*, involving *vab-3* (*Pax6*), *lin-22* (*h*) and *lin-32* (*ato*) (Wrischnik and Kenyon, 1997; Chisolm and Horvitz, 1995; Zhang and Emmons, 1995; Zhao and Emmons, 1995), suggesting that this regulatory hierarchy may be very widely conserved.

The evolutionary relationship of Math, Xath5 and ato

We have used three criteria, gene structure, expression and function, to test the orthology of Math5, Xath5 and ato. These three proteins share 100% amino acid identity of their basic DNA-binding domains. Domain swapping experiments between *Drosophila* ato and scute have demonstrated that basic domain amino acid composition confers neuron-type specificity (Chien et al., 1996). Therefore, complete conservation of Math5, Xath5 and ato basic domains implies that they function analogously. In the *Drosophila* compound eye, *ato* is expressed prior to R8 cell differentiation (Jarman et al., 1994). Similarly, *Math5* and *Xath5* are expressed prior to RGC formation. In each case, expression precedes differentiation of the first neuronal cell type, and it is tempting to speculate that these genes function orthologously in eye formation. However, it is important to be cautious (Abouheif, 1997) since, outside the eye, the expression patterns diverge.

Another test of orthology is gene function. In the fly eye, ectopic ato expression causes an increase in neuronal differentiation, with an excess of R8 photoreceptors (Dokucu et al., 1996). Ectopic expression of *Math5*, *Xath5* and *ato* in *Xenopus* embryos promotes neurogenesis (Fig. 5A; Kanekar et al., 1997; S. K. and M. L. V., unpublished observations). Lipofection of *ato* and *Xath5* into the *Xenopus* eye causes a significant bias towards RGC fate (Kanekar et al., 1997 and S. K. and M. L. V., unpublished observations). However, overexpression of *Math5* by lipofection in the frog retina results in a bias towards bipolar cell formation. Therefore, more comparisons of gene function are required to resolve the orthology issue. We are currently removing *Math5* function in mice by gene knockout to assess whether RGCs or other retinal neurons are affected. It will also be important to test whether *Math5* and/or *Xath5* rescue the *ato* mutant phenotype, and to compare *Math5*, *Xath5* and *ato* overexpression in mammalian tissues or cells.

The role of Math5 in retinal development

Math5 expression coincides with critical cellular events in the mammalian optic cup. The spread of *Math5* expression from the dorsal cup circumferentially toward ventral matches the progression of RGC layer formation between E12.5 and E13.5 (Hinds and Hinds, 1974; Young, 1983, 1985). However, the columns of *Math5*-expressing cells (Fig. 2F-H) do not correlate with previously described retinal structures. These cells may be clonally related (Turner et al., 1987) and/or represent 'proneural' clusters, analogous to groups of retinal precursors that express *ato* in the morphogenetic furrow (Jarman et al., 1993). Other vertebrate genes with a similar expression pattern are *Notch* and *Delta* (Dorsky et al., 1995, 1997; Henrique et al., 1997). It will be interesting to compare *Math5*, *Notch* and *Delta* expression domains to test whether they are complementary and to test for *Notch* or *Delta* regulation of *Math5*. Lastly, *Math5* expression is not observed in differentiated retinal neurons but instead, *Math5* mRNA is restricted to dividing progenitors (Fig. 2H). This observation, coupled with the ability of *Math5* to promote neuron formation (Figs 5, 6), suggests that *Math5* functions as a determination

factor, possibly to specify a particular retinal neuron class like RGCs, rather than during terminal differentiation. Paradoxically, *Math5* expression is excluded from the presumptive ciliary body, known to be highly proliferative (Young, 1985). However, cell division within the ciliary proliferative and the retinal ventricular zones may not be equivalent. The proliferating, undifferentiated margins of the vertebrate eye (ciliary marginal zone or presumptive ciliary body) are not unlike the region ahead of and within the morphogenetic furrow of a *Drosophila* eye imaginal disc. The presence of single *Math5*-positive cells adjacent to this region (Fig. 2E) and the correlation of several classes of transcription factors in the frog ciliary margin (Perron et al., 1998) circumstantially support this idea.

Given the sequence conservation, evolutionary relationship and similarity of retinal expression patterns for *Math5* and *Xath5*, our finding that ectopic *Math5* expression does not promote RGC fate in the frog retina was unexpected. There are several possible explanations for this result. First, *Math5* may play a role in regulating bipolar cell differentiation, although the timing of *Math5* expression relative to bipolar cell genesis argues against this. Second, *Math5* and *Xath5* may function analogously, but Math5 protein is incompletely active or relatively less stable in *Xenopus* retinal progenitor cells. For example, differences in stability, nuclear localization and myogenic potency have been observed between frog and mouse MyoD proteins in *Xenopus* microinjection experiments (Rupp et al., 1994). A cofactor interaction may also be required, which depends on amino acid residues that are less well conserved between Math5 and Xath5. Domain swap experiments between Xath5 and Math5 proteins may identify regions of Math5 that cause the retinal expansion and bipolar phenotypes.

Lastly, Math5 may produce a dominant-negative or dyschronic effect, particularly if it is subfunctional in *Xenopus* retinal cells. This possibility is supported by the expanded retinal phenotype and disruption of retinal organization noted in embryos injected with *Math5* RNA at the 16-cell stage (Fig. 5B). Overexpression of *Math5* may delay the differentiation of retinal progenitor cells. Then, as the retina matures and exogenous Math5 protein is degraded, progenitors may be released to differentiate as late-born neurons, e. g. bipolar cells. In this way, *Math5* may antagonize the action of endogenous *Xath5* to promote RGC formation. In spite of this apparent functional difference between *Xath5* and *Math5* in the *Xenopus* retinal lipofection assay, cells overexpressing *Math5* in 16-cell-injected embryos are NCAM-positive, even though they do not form normal retinal cell layers. Both Math5 and Xath5 promote neuron formation during neural plate formation, a general test of proneural activity. However, their ectopic expression affected retinal development differently in two separate experiments within the forming frog eye. Thus, future studies will focus on examining the underlying causes of these retinal phenotypes. Taken together, our findings suggest a role for Math5 as an intrinsic factor guiding the commitment of mammalian retinal progenitors and raise the possibility that mechanistic aspects of retinogenesis, like eye pattern formation in general may be evolutionarily conserved.

We are grateful to Jack Favor and Richard Maas for providing *Sey^{Neu}* mice, Jeremy Nathans for the P3-P7 eye cDNA library and François Guillemot for *Mash1*, *NeuroD*, *Ngn2/Math4A* and *Hes1* cDNA clones. We especially thank Grant Mastick for providing Pax6 antibody, assistance with antibody experiments and valuable discussions throughout the course of this work. We thank Yuh Nung Jan for his suggestion to search for Xath5-related genes in mice, John Kuwada for the use of his microscope and video capture equipment, Bill Harris for NCAM antibody, Peter Lalley for somatic cell hybrid DNA samples, Margit Burmeister for helpful discussion, Chuan-Min Chen and Vicki Kule for technical assistance and Marilyn Gandy for secretarial help. This manuscript was greatly improved by critical reading from Jim Lauderdale, Steve Easter, David Turner and Greg Dressler. This work was supported by grants from the American Cancer Society to M. L. V. (IRG 178F), the National Science Foundation to P. K. T. (DEB9707451) and the National Institutes of Health to T. G. (EY11729). T. G. is an Assistant Investigator of the Howard Hughes Medical Institute.

Note added in proof

A new member of the *atonal* bHLH family highly related to *Math5* and *Xath5* has recently been identified in chicken and deposited in GenBank (accession number 2760443).

REFERENCES

Abouheif, E. (1997). Developmental genetics and homology: a hierarchical approach. *Trends Ecol. Evol.* **12,** 405-408.

Acharya, H. R., Dooley, C. M., Thoreson, W. B. and Ahmad, I. (1997). cDNA cloning and expression analysis of NeuroD mRNA in human retina. *Biochem. Biophys. Res. Commun.* **233,** 459-463.

Akazawa, C., Ishibashi, M., Shimizu, C., Nakanishi, S. and Kageyama, R. (1995). A mammalian helix-loop-helix factor structurally related to the product of *Drosophila* proneural gene *atonal* is a positive transcriptional regulator expressed in the developing nervous system. *J. Biol. Chem.* **270,** 8730-8738.

Alexiades, M. R. and Cepko, C. L. (1997). Subsets of retinal progenitors display temporally regulated and distinct biases in the fates of their progeny. *Development* **124,** 1119-1131.

Belecky-Adams, T., Tomarev, S., Li, H.-S., Ploder, L., McInnes, R. R., Sundin, O. and Adler, R. (1997). Pax-6, Prox1, and Chx10 homeobox gene expression correlates with phenotypic fate of retinal precursor cells. *Invest. Ophth. Vis. Sci.* **38,** 1293-1303.

Ben-Arie, N., McCall, A. E., Berkman, S., Eichele, G., Bellen, H. J. and Zoghbi, H. (1996). Evolutionary conservation of sequence and expression of the bHLH protein Atonal suggests a conserved role in neurogenesis. *Hum. Mol. Genet.* **5,** 1207-1216.

Brown, N. L., Paddock, S. W., Sattler, C. A., Cronmiller, C., Thomas, B. J. and Carroll, S. B. (1996). *daughterless* is required for *Drosophila* photoreceptor cell determination, eye morphogenesis, and cell cycle progression. *Dev. Biol.* **179,** 65-78.

Brown, N. L., Sattler, C. A., Paddock, S. W. and Carroll, S. B. (1995). Hairy and Emc negatively regulate morphogenetic furrow progression in the *Drosophila* eye. *Cell* **80,** 879-887.

Campuzano, S. and Modolell, J. (1992). Patterning of the *Drosophila* nervous system: the *achaete-scute* gene complex. *Trends Genet.* **8,** 202-208.

Carter-Dawson, L. D. and LaVail, M. M. (1979). Rods and cones in the mouse retina 1. Autoradiographic analysis of cell generation using tritiated thymidine. *J. Comp. Neurol.* **188,** 263-272.

Cau, E., Gradwohl, G., Fode, C. and Guillemot, F. (1997). Mash1 activates a cascade of bHLH regulators in olfactory neuron progenitors. *Development* **124,** 1611-1621.

Caudy, M., Grell, E. H., Dambly-Chaudiere, C., Ghysen, A., Jan, L. Y. and Jan, Y. N. (1988). The maternal sex determination gene *daughterless* has zygotic activity necessary for the formation of peripheral neurons in *Drosophila*. *Genes Dev.* **2,** 843-852.

Cepko, C. L., Austin, C. P., Yang, X., Alexiades, M. and Ezzeddine, D. (1996). Cell fate determination in the vertebrate retina. *Proc. Nat. Acad. Sci. USA* **93,** 589-595.

Chien, C.-T., Hsiao, C.-D., Jan, L. Y. and Jan, Y. N. (1996). Neuronal type

information encoded in the basic helix-loop-helix domain of proneural genes. *Proc. Nat. Acad. Sci. USA* **93,** 13239-13244.

Chisolm, A.D. and Horvitz, H.R. (1995). Patterning of the *Caenorhabditis elegans* head region by the *Pax-6* family member, *vab-3*. *Nature* **377,** 52-55.

Cronmiller, C., Schedl, P. and Cline, T. W. (1988). Molecular characterization of *daughterless*, a *Drosophila* sex determination gene with multiple roles in development. *Genes Dev.* **2,** 1666-1676.

Cvekl, A. and Piatigorsky, J. (1996). Lens development and crystallin gene expression: many roles for *Pax-6*. *BioEssays* **18,** 621-630.

Davis, J. A. and Reed, R. L. (1996). Role of Olf-1 and Pax-6 transcription factors in neurodevelopment. *J. Neurosci.* **16,** 5082-5094.

del Rio, J. A. and Soriano, E. (1989). Immunocytochemical detection of 5′-bromodeoxyuridine incorporation in the central nervous system of the mouse. *Brain Res. Dev. Brain Res.* **49**, 311-317.

Desplan, C. (1997). Eye development: governed by dictator or junta? *Cell* **91,** 861-864.

Dokucu, M. E., Zipursky, S. L. and Cagan, R. L. (1996). Atonal, Rough, and the resolution of proneural clusters in the developing *Drosophila* retina. *Development* **122,** 4139-4147.

Dorsky, R. I., Rapaport, D. H. and Harris, W. A. (1995). *Xotch* inhibits cell differentiation in the Xenopus retina. *Neuron* **14**, 487-496.

Dorsky, R. I., Chang, W. S., Rapaport, D. H. and Harris, W. A. (1997). Regulation of neuronal diversity in the *Xenopus* retina by Delta signalling. *Nature* **385**, 67-70.

Erkman, L., McEvilly, R. J., Luo, L., Ryan, A. K., Hooshmand, F., O'Connell, S. M., Keithley, E. M., Rapaport, D. H., Ryan, A. F. and Rosenfeld, M. G. (1996). Role of transcription factors Brn-3.1 and Brn-3.2 in auditory and visual system development. *Nature* **381,** 603-606.

Ferreiro, B., Skoglund, P., Bailey, A., Dorsky, R. and Harris, W. A. (1992). XASH1, a Xenopus homolog of *achaete-scute*: A proneural gene in anterior regions of the vertebrate CNS. *Mech. Dev.* **40,** 25-36.

Fujiwara, M., Uchida, T., Osumi-Yamashita, N. and Eto, K. (1994). *Uchida* rat (rSey): a new mutant rat with craniofacial abnormalities resembling those of the mouse *Sey* mutant. *Differentiation* **57,** 31-38.

Furukawa, T., Kozak, C. A. and Cepko, C. L. (1997a). *rax*, a novel paired-type homeobox gene, shows expression in the anterior neural fold and developing retina. *Proc. Nat. Acad. Sci. USA* **94,** 3088-3093.

Furukawa, T., Morrow, E. M. and Cepko, C. L. (1997b). Crx, a novel otx-like homeobox gene, shows photoreceptor specific expression and regulates photoreceptor differentiation. *Cell* **91,** 531-541.

Ghysen, A., Dambly-Chaudiere, C., Jan, L. Y. and Jan, Y. N. (1993). Cell interactions and gene interactions in peripheral neurogenesis. *Genes Dev.* **7,** 723-733.

Glaser, T., Lane, J. and Housman, D. (1990). A mouse model of the Aniridia-Wilms tumor deletion syndrome. *Science* **250,** 823-827.

Glaser, T., Walton, D. S. and Maas, R. L. (1992). Genomic structure, evolutionary conservation and aniridia mutations in the human Pax6 gene. *Nat. Genet.* **2,** 232-239.

Glaser, T., Jepeal, L., Edwards, J. G., Young, S. R., Favor, J. and Maas, R. L. (1994). PAX6 gene dosage effect in a family with congenital cataracts, aniridia, anophthalmia and central nervous system defects. *Nat. Genet.* **7**, 463-471.

Gradwohl, G., Fode, C. and Guillemot, F. (1996). Restricted expression of a novel murine *atonal*-related bHLH protein in undifferentiated neural precursors. *Dev. Biol.* **180,** 227-241.

Grindley, J. C., Davidson, D. R. and Hill, R. E. (1995). The role of Pax-6 in eye and nasal development. *Development* **121,** 1433-1442.

Guillemot, F. and Cepko, C. (1992). Retinal fate and ganglion cell differentiation are potentiated by acidic FGF in an in vitro assay of early retinal development. *Development* **114,** 743-754.

Guillemot, F. and Joyner, A. L. (1993). Dynamic expression of the murine Achaete-Scute homologue Mash-1 in the developing nervous system. *Mech. Dev.* **42,** 171-185.

Guillemot, F., Lo, L.-C., Johnson, J., Auerbach, A., Anderson, D. J. and Joyner, A. L. (1993). Mammalian achaete-scute homolog 1 is required for the early development of olfactory and autonomic neurons. *Cell* **75,** 463-476.

Halder, G., Callaerts, P., Flister, S., Walldorf, U. and Gehring, W. J. (1998). *eyeless* initiates the expression of both *sine oculis* and *eyes absent* during *Drosophila* compound eye development. *Development* **125,** 2181-2191.

Halder, G., Callaerts, P. and Gehring, W. J. (1995). New perspective on eye evolution. *Curr. Biol.* **5,** 602-609.

Hanson, I. and van Heyningen, V. (1995). Pax6: more than meets the eye. *Trends. Genet.* **11,** 268-272.

Hargrave, M. and Koopman, P. (1998). In situ hybridization of whole mouse embryos. In *In Situ Hybridization Protocols* (ed. I. Darby). Humana Press, Totowa, NJ (in press).

Harland, R. (1991). In situ hybridization: an improved whole-mount method for *Xenopus* embryos. *Methods Cell Biol.* **36,** 685-695.

Henrique, D., Hirsinger, E., Adam, J., Le Roux, I., Pourquie, O., Ish-Horowicz, D. and Lewis, J. (1997). Maintenance of neuroepithelial progenitor cells by Delta-Notch signalling in the embryonic chick retina. *Current Biol.* **7**, 661-670.

Hill, R. E. , Favor, J., Hogan, B. L., Ton, C. C., Saunders, G. F., Hanson, I. M., Prosser, J., Jordan, T., Hastie, N. D. and van Heyningen, V. (1991). Mouse *Small eye* results from mutations in a paired-like homeobox-containing gene. *Nature* **354,** 522-525.

Hinds, J. W. and Hinds, P. L. (1974). Early ganglion cell differentiation in the mouse retina: An electron microscopic analysis utilizing serial sections. *Dev. Biol.* **37,** 381-416.

Hogan, B. L. M., Horsburgh, G., Cohen, J., Hetherington, C. M., Fisher, G. and Lyon, M. F. (1986). *Small eyes (Sey)*: a homozygous lethal mutation on chromosome 2 which affects the differentiation of both lens and nasal placodes in the mouse. *J. Embry. Exp. Morph.* **97,** 95-110.

Holt, C. E., Bertsch, T. W., Ellis, H. M. and Harris, W. A. (1988). Cell determination in the *Xenopus* retina is independent of lineage and birth date. *Neuron* **1,** 15-26.

Huang, S. and Moody, S. A. (1993). The retinal fate of Xenopus cleavage stage progenitors is dependent upon blastomere position and competence: studies of normal and regulated clones. *J. Neurosci.* **13,** 3193-3210.

Isaka, F., Shimizu, C., Shigetada, N. and Kageyama, R. (1996). Genetic mapping of four mouse bHLH genes related to *Drosophila* proneural gene *atonal*. *Genomics* **37,** 400-402.

Ishibashi, M., Ang, S.-L., Shiota, K., Nakanishi, S., Kageyama, R. and Guillemot, F. (1995). Targeted disruption of mammalian hairy and Enhancer of split homolog-1 (HES-1) leads to up-regulation of neural helix-lop-helix factors, premature neurogenesis, and severe neural tube defects. *Genes Dev.* **9,** 9136-9148.

Jan, Y. N. and Jan, L. Y. (1993). HLH proteins, fly neurogenesis, and vertebrate neurogenesis. *Cell* **75,** 827-830.

Jarman, A. P., Grau, Y., Jan, L. Y. and Jan, Y. N. (1993). *atonal* is a proneural gene that directs chordotonal organ formation in the *Drosophila* peripheral nervous system. *Cell* **73,** 1307-1321.

Jarman, A. P., Grell, E. H., Ackerman, L., Jan, L. Y. and Jan, Y. N. (1994). *atonal* is the proneural gene for *Drosophila* photoreceptors. *Nature* **369,** 398-400.

Jarman, A. P., Sun, Y., Jan, L. Y. and Jan, Y. N. (1995). Role of the proneural gene, *atonal*, in formation of *Drosophila* chordotonal organs and photoreceptors. *Development* **121,** 2019-2030.

Jasoni, C. and Reh, T. (1996). Temporal and spatial pattern of MASH-1 expression in the developing rat retina demonstrates progenitor cell heterogeneity. *J. Comp. Neurol.* **369,** 319-327.

Johnson, J. E., Birren, S. J. and Anderson, D. J. (1990). Two rat homologues of *Drosophila achaete-scute* specifically expressed in neuronal precursors. *Nature* **346,** 858-861.

Kageyama, R., Sasai, Y., Akazawa, C., Makoto, I., Takebayashi, K., Shimizu, C., Tomita, K. and Nakanishi, S. (1995). Regulation of mammalian neural development by helix-loop-helix transcription factors. *Crit. Rev. Neurobiol.* **9,** 177-188.

Kanekar, S., Perron, M., Dorsky, R., Harris, W. A., Jan, L. Y., Jan, Y. N. and Vetter, M. L. (1997). *Xath5* participates in a network of bHLH genes in the developing *Xenopus* retina. *Neuron* **19,** 981-994.

Koroma, B. M., Yang, J.-M. and Sundin, O. H. (1997). The Pax-6 homeobox gene is expressed throughout the corneal and conjunctival epithelia. *Invest. Ophth. Vis. Sci.* **38,** 108-120.

Kozak, M. (1989). The Scanning Model for Translation: An Update. *J. Cell Biol.* **108,** 229-241.

Laird, P. W., Zijderveld, A., Linders, K., Rudnicki, M. A., Jaenisch, R. and Berns, A. (1991). Simplified mammalian DNA isolation procedure. *Nucl. Acids Res.* **19,** 4293.

Lalley, P. A., Francke, U. and Minna, J. D. (1978). Homologous genes for enolase, phosphogluconate dehydrogenase, phophoglucomutase, and adenylate kinase are syntenic on mouse chromosome 4 and human chromosome 1p. *Proc. Nat. Acad. Sci. USA* **75,** 2382-2386.

Lee, J. (1997). Basic helix-loop-helix genes in neural development. *Curr. Op. Neuro.* **7,** 13-20.

Lee, J. E., Hollenberg, S. M., Snider, L., Turner, D. L., Lipnick, N. and Weintraub, H. (1995). Conversion of *Xenopus* ectoderm into neurons by NeuroD, a basic helix-loop-helix protein. *Science* **268,** 836-844.

Loster, J., Immervoll, T., Schmitt-John, T. and Graw, J. (1997). *Cat3^{vl}* and *Cat^{vao}* cataract mutations on mouse chromosome 10: phenotypic characterization, linkage studies and analysis of candidate genes. *Mol. Gen. Genet.* **275,** 95-102.

Ma, Q., Chen, Z., Barrantes, I., de la Pompa, J. L. and Anderson, D. J. (1998). neurogenin1 is essential for the determination of neuronal precursors for proximal cranial sensory ganglia. *Neuron* **20,** 469-482.

Ma, Q., Kintner, C. and Anderson, D. J. (1996). Identification of *neurogenin*, a vertebrate determination gene. *Cell* **87,** 43-52.

Mastick, G. M., Davis, N. M., Andrews, G. L. and Easter, S. S. (1997). Pax6 functions in boundary formation and axon guidance in the embryonic mouse forebrain. *Development* **124,** 1985-1997.

Mathers, P. H., Grinbery, A., Mahon, K. A. and Jamrich, M. (1997). The Rx homeobox gene is essential for vertebrate eye development. *Nature* **387,** 603-607.

Moody, S. A. (1987). Fates of the blastomeres of the 16-cell stage *Xenopus* embryo. *Dev. Biol.* **119,** 560-578.

Ohsako, S., Hyer, J., Panganiban, G., Oliver, I. and Caudy, M. (1994). *hairy* function as a DNA-binding HLH repressor of *Drosophila* sensory organ formation. *Genes Dev.* **8,** 2743-2755.

Park, C. M. and Hollenberg, M. J. (1989). Basic fibroblast growth factor induces retinal regeneration in vivo. *Dev. Biol.* **134,** 201-205.

Perron, M., Kanekar, S., Vetter, M. L. and Harris, W. A. (1998). The genetic sequence of retinal development in the ciliary margin of the Xenopus eye. *Dev. Biol.* **199**, 185-200.

Pittack, C., Jones, M. and Reh, T. A. (1991). Basic fibroblast growth factor induces retinal pigment epithelium to generate neural retina in vitro. *Development* **113,** 577-588.

Porter, F. D., Drago, J., Xu, Y., Cheema, S. S., Wassif, C., Huang, S. P., Lee, E., Grinberg, A., Massalas, J. S., Bodine, D., Alt, F. and Westphal, H. (1997). *Lhx2*, a LIM homeobox gene, is required for eye, forebrain, and definitive erythrocyte development. *Development* **124,** 2935-2944.

Reddy, G. V., Gupta, B., Ray, K. and Rodrigues, V. (1997). Development of the *Drosophila* olfactory sense organs utilizes cell-cell interactions as well as lineage. *Development* **124,** 703-712.

Richter, K., Grunz, H. and Dawid, I. B. (1988). Gene expression in the embryonic nervous system of *Xenopus laevis*. *Proc. Nat. Acad. Sci. USA* **85,** 8086-8090.

Robinson, S. R. (1991). Development of the Mammalian Retina. In *Neuroanatomy of the Visual Pathways and Their Development* (ed. B. Dreher and S. R. Robinson), Vol. 3, pp. 69-149.

Roztocil, T., Matter-Sadzinski, L., Alliod, C., Ballivet, M. and Matter, J.-M. (1997). *NeuroM*, a neural helix-loop-helix transcription factor, defines a new transition state in neurogenesis. *Development* **124,** 3263-3272.

Rupp, R. A. W., Snider, L. and Weintraub, H. (1994). *Xenopus* embryos regulate the nuclear localization of *XMyoD*. *Genes Dev.* **8,** 1311-1323.

Sakaguchi, D. S., Moeller, J. F., Coffman, C. R., Gallenson, N. and Harris, W. A. (1989). Growth cone interactions with a glial cell line from embryonic *Xenopus* retina. *Dev. Biol.* **134,** 158-174.

Sasai, Y., Kageyama, R., Tagawa, Y., Shigemoto, R. and Nakanishi, S. (1992). Two mammalian helix-loop-helix factors structurally related to *Drosophila hairy* and *Enhancer of split*. *Genes Dev.* **6,** 2620-2634.

Satakato, I. and Maas, R. (1994). Msx1 deficient mice exhibit cleft palate and abnormalities of craniofacial and tooth development. *Nat. Genet.* **6,** 348-356.

Schaeren-Weimers, N. and Gerfin-Moser, A. (1993). A single protocol to detect transcripts of various types and expression levels in neural tissue and cultured cells: in situ hybridization using digoxigenin-labeled cRNA probes. *Histochemistry* **100,** 431-440.

Schedl, A., Ross, A., Lee, M., Engelkamp, D., Rashbass, P., van Heynigen, V. and Hastie, N. D. (1996). Influence of PAX gene dosage on development: overexpression causes severe eye abnormalities. *Cell* **86**, 71-82.

Shimizu, C., Akazawa, C., Nakanishi, N. and Kageyama, R. (1995). *Math-2*, a mammalian helix-loop-helix factor structurally related to the product of *Drosophila* proneural gene *atonal*, is specifically expressed in the nervous system. *Eur. J. Biol.* **229,** 239-248.

Sommer, L., Ma, Q. and Anderson, D. J. (1996). *neurogenins*, a novel family of *atonal*-related bHLH transcription factors, are putative mammalian neuronal determination genes that reveal progenitor cell heterogeneity in the developing CNS and PNS. *Mol. Cell. Neuro.* **8,** 221-241.

Swofford, D. L. (1993). PAUP: phylogenetic analysis using parsimony, version 3.1.1. In *Illinois Natural History Survey.* Champaign, Illinois.

Takebayashi, K., Takahashi, S., Yokota, C., Tsuda, H., Nakanishi, S., Asashima, M. and Kageyama, R. (1997). Conversion of ectoderm into a neural fate by ATH-3, a vertebrate basic helix-loop-helix gene homologous to *Drosophila* proneural gene *atonal*. *EMBO J.* **16,** 384-395.

Theiler, K., Varnum, D. S. and Stevens, L. C. (1978). Development of Dickie's small eye, a mutation in the house mouse. *Anat. Embryol.* **155,** 81-86.

Tomita, K., Nakanishi, S., Guillemot, F. and Kageyama, R. (1996a). Mash1 promotes neuronal differentiation in the retina. *Genes to Cells* **1**, 765-774.

Tomita, K., Ishibashi, M., Nakahara, K., Ang, S.-L., Nakanishi, S., Guillemot, F. and Kageyama, R. (1996b). Mammalian hairy and Enhancer of split homolog 1 regulates differentiation of retinal neurons and is essential for eye morphogenesis. *Neuron* **16,** 723-734.

Ton, C. C., Hirvonen, H., Miwa, H., Weil, M. M., Monaghan, P., Jordan, T., van Heyningen, V., Hastie, N. D., Meijers-Heijboer, H., Dreschler, M. et al. (1991). Positional cloning and characterization of a paired box- and homeobox-containing gene from the Aniridia region. *Cell* **67,** 1059-1074.

Turner, D. L., Snyder, E. Y. and Cepko, C. L. (1987). A common progenitor for neurons and glia persists in rat retina late in development. *Neuron* **4,** 833-845.

Turner, D. L. and Weintraub, H. (1994). Expression of *achaete-scute* homolog 3 in *Xenopus* embryos converts ectodermal cells to a neural fate. *Genes Dev.* **8,** 1434-1447.

Van Doren, M., Bailey, A. M., Esnayra, J., Ede, K. and Posakony, J. W. (1994). Negative regulation of proneural gene activity: *hairy* is a direct transcriptional repressor of *achaete*. *Genes Dev.* **8,** 2729-2742.

Van Doren, M., Ellis, H. and Posakony, J. W. (1991). The *Drosophila* extramacrochaetae protein antagonizes sequence-specific DNA binding by daughterless/achaete-scute protein complexes. *Development* **113,** 245-255.

Walther, C. and Gruss, P. (1991). Pax-6 a murine paired box gene, is expressed in the developing CNS. *Development* **113,** 1435-1449.

Wantanabe, T. and Raff, M. C. (1990). Rod photoreceptor development in vitro: Intrinsic properties of proliferating neuroepithelial cells change as development proceeds in the rat retina. *Neuron* **2,** 461-467.

Wetts, R. and Fraser, S. E. (1988). Multipotent precursors can give rise to all major cell types of the frog retina. *Science* **239,** 1142-1145.

Wetts, R., Kook, J. H. and Fraser, S. E. (1993). Proportion of proliferative cells in the tadpole retina is increased after embryonic lesion. *Dev. Dynam.* **198**, 54-64.

Williams, R. W. and Goldowitz, D. (1992). Lineage versus environment in embryonic retina: a revisionist perspective. *Trends. Genet.* **15,** 368-373.

Wrischnik, L. A. and Kenyon, C. J. (1997). The role of *lin22*, a *hairy/Enhancer of split* homolog, in patterning the peripheral nervous system of *C. elegans*. *Development* **124,** 2875-2888.

Xu, P.-X., Woo, I., Her, H., Beier, D. R. and Maas, R. L. (1997). Mouse *Eya* homologues of the *Drosophila eyes absent* gene require *Pax6* for expression in lens and nasal placode. *Development* **124,** 219-231.

Young, R. W. (1983). The life history of retinal cells. *Trans. Am. Ophthalmol. Soc.* **81,** 193-228.

Young, R. W. (1985). Cell proliferation during postnatal development of the retina in the mouse. *Brain Research* **353,** 229-239.

Zhang, Y. and Emmons, S. W. (1995). Specification of sense-organ identity by a *Caenorhabditis elegans Pax-6* homologue. *Nature* **377,** 55-59.

Zhao, C. and Emmons, S. W. (1995). A transcription factor controlling development of peripheral sense organs in C. elegans. *Nature* **373,** 74-78.